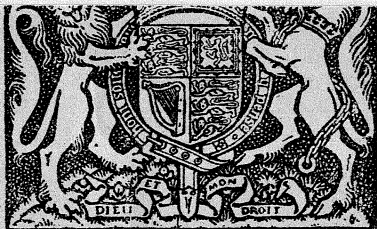


R&M 1838  
R5672



## AIR MINISTRY

AERONAUTICAL RESEARCH COMMITTEE  
REPORTS AND MEMORANDA

# The Calculation of the Profile Drag of Aerofoils

*By*

H. B. SQUIRE, M.A. AND A. D. YOUNG, B.A.



*Crown Copyright Reserved*

LONDON : HIS MAJESTY'S STATIONERY OFFICE

Price 4s. od. net

R&M 1838



3 8006 10054 7069

# The Calculation of the Profile Drag of Aerofoils

By

H. B. SQUIRE, M.A. and A. D. YOUNG, B.A.

COMMUNICATED BY THE DIRECTOR OF SCIENTIFIC RESEARCH, AIR MINISTRY

*Reports and Memoranda No. 1838*  
*18th November, 1937\**

**SUMMARY.**—Owing to improvements in aerodynamic design it is desirable to be able to predict profile drag accurately. A method of calculating the profile drag of aerofoils is developed and is applied to investigate the drag of a flat plate and of two aerofoils of different thicknesses for three Reynolds numbers and three transition point positions.

From the results curves are drawn which show the variation of profile drag for a range of aerofoil thickness, Reynolds number and transition point position. Comparison with experimental results shows satisfactory agreement.

## CONTENTS

	Page
1. Introduction .....	2
2. Preliminary discussion .....	2
3. Details of method .....	5
3.1. Pressure distribution .....	5
3.2. Laminar layer .....	5
3.3. The transition point .....	6
3.4. Turbulent layer .....	7
3.5. Wake .....	9
4. Details of calculations .....	12
4.1. Cases considered .....	12
4.2. Results of calculations .....	14
4.3. Accuracy .....	20
5. Comparison with experiment .....	21
6. Extensions of the theory .....	22
7. Appendix I. Derivation of equation (9) .....	23
8. Appendix II. Factors controlling transition .....	24
9. Appendix III. Pressure gradients across the boundary layer .....	25
10. Appendix IV. Notation .....	26
List of References .....	27

\* R.A.E. Report, November, 1937.

1. *Introduction.*—Owing to the improvement in aerodynamic design in recent years the accurate determination of the profile drag of aerofoils has become important and a satisfactory method of calculating profile drag is desirable.

For smooth aerofoils the three most important parameters which affect the profile drag are the wing thickness, Reynolds number and transition point position. Other parameters which may affect profile drag are section shape and lift coefficient; but the actual shape does not differ greatly for different modern sections and the lift coefficient for top speed conditions does not vary over a wide range, so that the effect of varying these two parameters is unlikely to be very important. The method of calculating profile drag developed below has therefore been applied only to typical wing sections at a single value of the lift coefficient.

2. *Preliminary discussion.*—Profile drag consists partly of skin friction, which arises from the tangential stresses at the surface of the aerofoil, and partly of form drag, which arises from the normal pressures. For streamline bodies the pressure distribution closely resembles the pressure distribution corresponding to potential flow, which, apart from induced drag, has no resultant along the direction of motion. The distortion of the pressure distribution from the potential pressure distribution is due to the boundary layer, which increases in thickness from the leading edge to the trailing edge and reduces the pressure towards the trailing edge. Thus the form drag of a streamline body is due to the boundary layer and can be determined if the development of the boundary layer and the wake can be properly analysed.

Consider the two-dimensional flow past a streamline cylinder as shown in Fig. 1. The total pressure is constant in the fluid field except in the boundary layer and in the wake, which are shown shaded. Starting from the stagnation point A, boundary layers are present on the upper and lower surfaces of the aerofoil. The boundary layers will generally be laminar for some distance and transition to

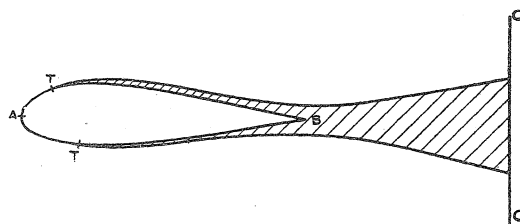


FIG. 1.

turbulence will begin at the points T (Fig. 1). After a transition region fully turbulent boundary layers are formed. At the trailing edge B the boundary layers of the upper and lower surfaces coalesce to form the wake, which extends downstream.

The wake has a minimum thickness a short distance downstream of the trailing edge and then becomes gradually broader. The static pressure in the wake is greatest at the trailing edge and decreases downstream, eventually becoming equal to the static pressure of the free stream. For a section of the wake CC sufficiently far downstream for this to be true it is easy to show, from momentum considerations, that the drag per unit length of the cylinder is given by

$$D = \rho \int_{-\infty}^{\infty} u (U_0 - u) dy \dots \dots \dots \quad (1)$$

where  $U_0$  is the velocity of the free stream,  $u$  is the velocity in the wake parallel to the direction of motion at a point of the measurement plane,  $y$  is measured normal to the direction of motion, and  $\rho$  is the density of the fluid; the integrand vanishes outside the wake since  $u$  is there equal to  $U_0$ .

The drag coefficient  $C_D$  of the aerofoil is defined by

$$D = C_D \cdot \frac{1}{2} \rho U_0^2 \cdot c$$

where  $c$  is the chord of the aerofoil. The momentum thickness of the wake far downstream is defined by

$$\theta_0 = \int_{-\infty}^{\infty} \frac{u}{U_0} \left(1 - \frac{u}{U_0}\right) dy \dots \dots \dots \quad (2)$$

Then from (1) we obtain

$$C_D = \frac{2}{c} \int_{-\infty}^{\infty} \frac{u}{U_0} \left(1 - \frac{u}{U_0}\right) dy = \frac{2\theta_0}{c} \dots \dots \dots \quad (3)$$

This relation shows that the drag coefficient of the aerofoil can be determined if the momentum thickness of the wake far downstream can be calculated.

If  $\tau_0$  is the skin friction at the surface of the aerofoil the skin friction drag coefficient  $C_f$  is given by

$$C_f = \frac{2}{c} \int \frac{\tau_0}{\rho U_0^2} d\xi \dots \dots \dots \dots \dots \quad (4)$$

where  $\xi$  is measured parallel to the direction of the free stream (account must be taken of the two surfaces of the aerofoil). In general  $C_f$  is less than  $C_D$ .

The above discussion is the basis of the analysis. With a given pressure distribution on an aerofoil section the development of the boundary layers is followed from the forward stagnation point. The boundary layers are assumed to be laminar for a certain distance, transition is assumed to occur suddenly, and the development of the fully turbulent boundary layers is then followed to the trailing edge; the distribution of the skin friction and of the boundary layer momentum thickness over the surface of the cylinder is thus obtained. The wake is investigated

on the assumption that its momentum thickness at the trailing edge is equal to the sum of the momentum thicknesses of the boundary layers of the upper and lower surfaces there. The value of the wake momentum thickness far downstream is derived from the momentum equation of the wake and the profile drag is then determined from equation (3).

Though the skin friction distribution over the surface is obtained incidentally, the profile drag calculated directly includes both skin friction and form drag, and the distinction between form drag and skin friction becomes to some extent artificial\*†.

In order to permit interpolation for a range of aerofoil thickness the flat plate at zero incidence and two aerofoils of thicknesses  $0.14c$  and  $0.25c$  were considered. These aerofoils are shown inset in Fig. 2 and 3.

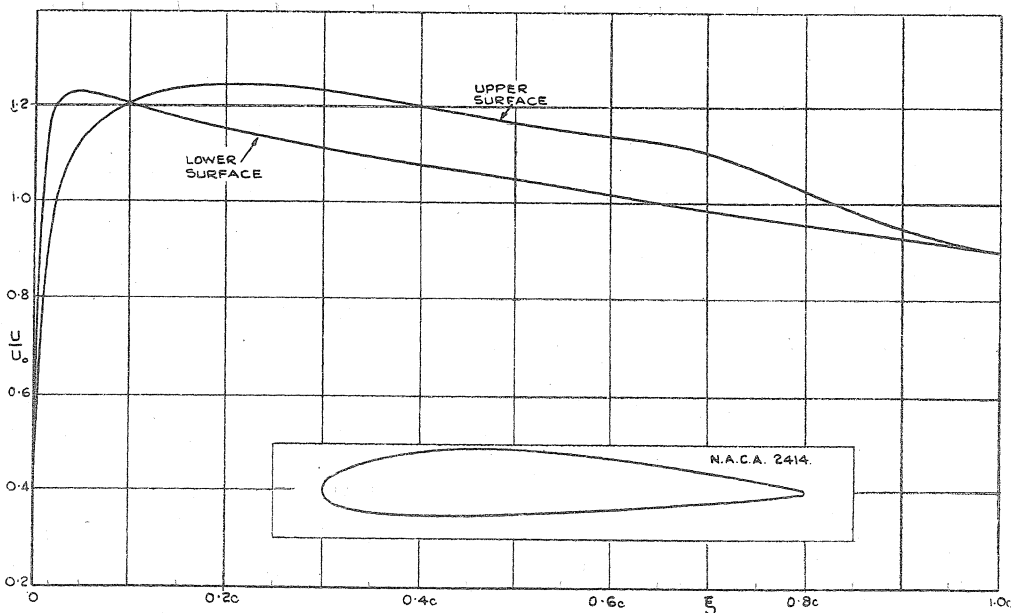


FIG. 2.—Velocity Distribution for Wing Section N.A.C.A. 2414.  $C_L = 0.18$ .

\* An attempt to determine the form drag of aerofoils was made by Professor B. M. Jones, who suggested, in an unpublished note, that the rate at which work is done on a fluid by a body moving through it is equal to  $\int \tau_0 U dx$ , where  $\tau_0$  is the surface friction,  $U$  is the velocity outside the boundary layer and  $x$  is measured along the surface. Professor G. I. Taylor showed, also in an unpublished note, that the formula given by Professor Jones was not exact except for a flat plate, and he deduced a formula for the necessary correction by application of the momentum equation of the boundary layer. In Professor Taylor's note the idea of the continuity of the wake with the boundary layers of the upper and lower surfaces of the aerofoil was first introduced. The analysis of the present report is developed on rather different lines from Professor Taylor's, but we are particularly indebted to him for this idea of the continuity of the boundary layers and the wake.

† The above discussion applies equally to the flow of compressible or incompressible fluids, provided that no shock waves are present.

*3. Details of method.* 3.1. *Pressure distribution.*—The thinner aerofoil was of section N.A.C.A. 2414 and was assumed to be at an incidence giving a lift coefficient of 0·18; the corresponding pressure distribution was obtained from the theory of potential flow<sup>1</sup>. The distribution given by this method was modified towards the trailing edge to make a rough allowance for the effect of the boundary layer in preventing a rapid rise in pressure there\*. The velocity distribution at

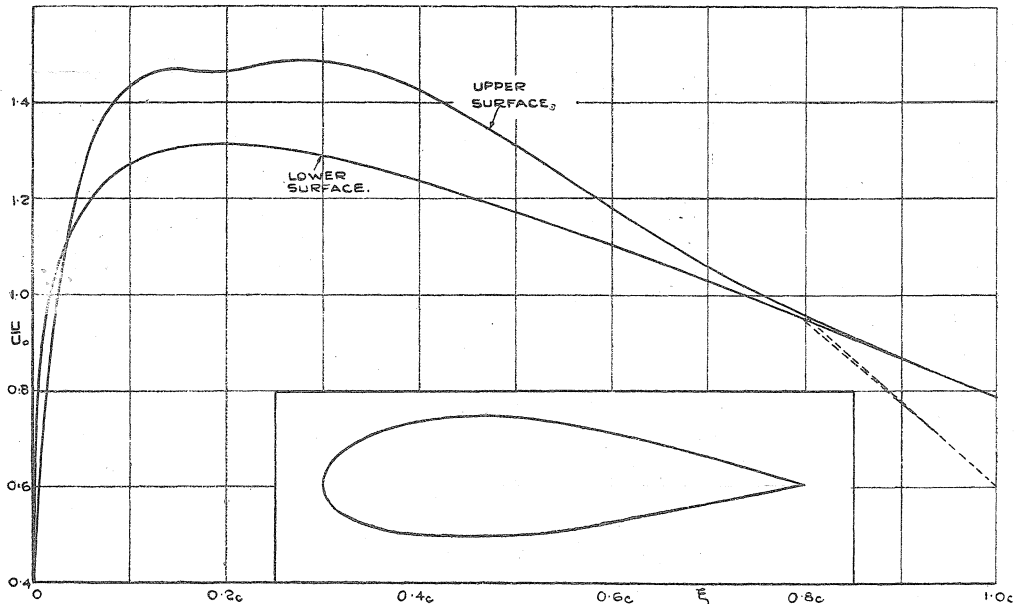


FIG. 3.—Velocity Distribution for 25 per cent. Thick Wing Section.  $C_L = 0\cdot25$ .

the outer edge of the boundary layer was then derived from Bernouilli's equation and is shown in Fig. 2.

The pressure distribution for the thicker aerofoil was measured experimentally in flight over the range 0·08c to 0·50c from the leading edge<sup>2</sup> and the distribution over the rest of the profile was faired in, after examination of the results of wind tunnel tests on pressure distributions\*; the corresponding velocity distribution at the edge of the boundary layer is shown in Fig. 3.

3.2. *Laminar layer.*—The skin friction and boundary layer thickness for the region of laminar flow near the leading edge were calculated by Pohlhausen's method<sup>3</sup>; this method requires the solution of the equation

$$\frac{dz}{dx} = \frac{f(\lambda)}{U} + U'' z^2 \cdot g(\lambda) \quad \dots \quad \dots \quad \dots \quad \dots \quad \dots \quad (5)$$

in which  $z = \delta^2/\nu$ ,  $\lambda = U' z$ ,

---

\* Experimental measurements of pressure downstream of the trailing edge, which had been made in the measurement of drag by the momentum method, were useful in determining the pressure at the trailing edge.

where  $x$  is the distance measured along the surface from the forward stagnation point,

$\delta$  is the boundary layer thickness,

$U$  is the velocity at the edge of the boundary layer,

$\nu$  is the kinematic viscosity of the fluid,

$f(\lambda)$  and  $g(\lambda)$  are functions which are tabulated in Reference 3, and dashes denote differentiation with respect to  $x$ . At the stagnation point  $x = 0$ ,  $\lambda$  is equal to 7.052. Equation (5) was solved by a step-by-step method for both surfaces up to the assumed transition points.

The skin friction at the surface is given by

$$\tau_0 = \frac{\mu(\lambda + 12) U}{6\delta}$$

and the local skin friction coefficient by

$$c_f = \frac{2\tau_0}{\rho U_0^2} = \frac{(\lambda + 12) \nu U}{3 \delta U_0^2}$$

As is usual for laminar boundary layers,  $c_f$  is proportional to  $R^{-1/2}$ , where  $R$  is the Reynolds number  $U_0 c / \nu$ . In addition, the momentum thickness of the laminar boundary layer, defined by

$$\theta = \int_0^\delta \frac{u}{U} \left(1 - \frac{u}{U}\right) dy$$

where  $u$  is the velocity in the layer parallel to the surface, and  $y$  is measured normal to the surface, is given by<sup>3</sup>

$$\frac{\theta}{\delta} = \frac{5328 - 48\lambda - 5\lambda^2}{45360} \quad \dots \dots \dots \quad (6)$$

It is now generally considered that Pohlhausen's method does not give a satisfactory solution of the laminar boundary layer equations in regions where the pressure is rising and in particular cannot be used to determine the separation point of the laminar layer<sup>4</sup>. In this report, however, we are not concerned directly with laminar separation and the errors introduced by incorrect representation of the laminar skin friction in the retarded region will be very small, since the skin friction in the retarded region is itself small. The error in the momentum thickness will also be small, since it is related to the integral of the skin friction.

3.3. *The transition point.*—Measurements of frictional intensity in wind tunnels of moderate turbulence suggested that the transition from laminar to turbulent

flow took place over a long distance<sup>5</sup>. More recent experiments in wind tunnels<sup>6</sup> and flight tests in the turbulence-free atmosphere<sup>7</sup> have shown that transition occurs suddenly and it is therefore permissible to assume that transition occurs at a point which will be referred to as the transition point\*.

The momentum thickness of the boundary layer must then be taken to be continuous and the skin friction to be discontinuous at this point; a discontinuity in the momentum thickness would require the introduction of a finite impulse at the transition point, whereas the skin friction, though not actually discontinuous, probably increases very rapidly over a short region near the transition point. Thus the value of  $\theta$ , given by (6), at the end of the laminar layer, will be the initial value of  $\theta$  at the beginning of the turbulent layer†.

**3.4. Turbulent layer.**—The boundary layer momentum equation, which is the basis of the analysis of both the laminar and turbulent layers, may be written<sup>8</sup>

$$\tau_0 = \frac{d M}{dx} - \delta^* \frac{dp}{dx} \dots \dots \dots \dots \dots \quad (7)$$

in which  $M = \rho U^2 \theta = \rho \int_0^\delta u (U - u) dy$

and  $\delta^* = \int_0^\delta (1 - \frac{u}{U}) dy$

where  $x$  is the distance measured along the surface from the forward stagnation point,

$y$  is measured normal to the surface,

$p$  is the pressure in the boundary layer,

$U$  is the velocity at the edge of the boundary layer,

$u$  is the velocity in the boundary layer parallel to the surface,

$\tau_0$  is the local surface friction,

$M$  is a measure of the momentum defect in the boundary layer,

$\theta$  is the momentum thickness,

and  $\delta^*$  is the displacement thickness.

By Bernouilli's equation, which holds at the edge of the boundary layer,

$$\frac{dp}{dx} = - \rho U \frac{dU}{dx} .$$

\* Owing to wind tunnel turbulence the transition point may move rapidly to and fro so that instruments measuring mean values would indicate that transition to turbulence occurred gradually in some wind tunnels.

† A note on the factors governing transition is given in Appendix II.

Substituting in (7) we obtain

$$\frac{\tau_0}{\rho U^2} = \frac{d\theta}{dx} + \frac{U'}{U} (H + 2)\theta \quad \dots \quad \dots \quad \dots \quad \dots \quad \dots \quad (8)$$

where  $H = \delta^x/\theta$ , and dashes denote differentiation with respect to  $x$ .

It is necessary to find a relation between  $\tau_0$ ,  $U$  and  $\theta$  which is valid for turbulent boundary layers. To derive such a relation we assume that the same relation holds between the local values of these quantities as holds for a flat plate with fully turbulent boundary layer. This is equivalent to assuming that the pressure gradients at the surface of an aerofoil do not affect the velocity distribution in the turbulent layer, and is an approximation which may be sufficiently accurate for the small pressure gradients present in the cases considered. For the flat plate with fully turbulent boundary layer this relation is represented closely by the equation

$$\frac{U\theta}{v} = 0.2454 e^{0.3914\zeta} \quad \dots \quad \dots \quad \dots \quad \dots \quad \dots \quad \dots \quad (9)$$

where  $\zeta^2 = \rho U^2 / \tau_0$ . The derivation of this formula is given in Appendix I.

Assuming that (9) holds for the turbulent boundary layer of an aerofoil we substitute in the momentum equation (8) and obtain

$$\frac{d\zeta}{dx} + 2.557 (H + 1) \frac{U'}{U} = \frac{10.411 U e^{-0.3914\zeta}}{v\zeta^2} \quad \dots \quad \dots \quad \dots \quad (10)$$

To determine  $H$  we use the experimental results of Nikuradse and Buri<sup>9</sup> on flow in diverging and converging channels, which indicate that it is sufficiently accurate to assume that  $H$  is constant and equal to 1.4. With this value for  $H$  equation (10) becomes

$$\frac{d\zeta}{dx} + 6.13 \frac{U'}{U} = \frac{U}{v} F(\zeta) \quad \dots \quad \dots \quad \dots \quad \dots \quad \dots \quad (11)$$

where  $F(\zeta) = 10.411 \zeta^{-2} e^{-0.3914\zeta}$ ; numerical values of  $F(\zeta)$  are given in Table 1.

TABLE 1

$\zeta$	$10^6 F(\zeta)$	$\zeta$	$10^6 F(\zeta)$
14	221.6	24	1.502
15	130.39	25	0.937
16	77.47	26	0.585
17	46.11	27	0.367
18	27.97	28	0.2308
19	16.96	29	0.1454
20	10.35	30	0.0917
21	6.35	31	0.0582
22	3.908	32	0.0369
23	2.418	33	0.0235

Equation (11) can be solved by a step-by-step method if  $U$  is known as a function of  $x$  and the value of  $\zeta$  at the transition point is also known\*. To determine the initial values of  $\zeta$  we take the value of  $\theta$  for the laminar layer at the assumed transition point, which is given by (6), and determine the corresponding value of  $\zeta$  from (9), which may be written

$$\zeta = 2.557 \log_e (4.075 \frac{U\theta}{v})$$

The solution of (11) for any particular case gives the skin friction distribution from the relation  $\zeta^2 = \rho U^2 / \tau_0$ , and the distribution of  $\theta$  along the surface is derived from (9). The sum of the values of  $\theta$  corresponding to the upper and lower surfaces gives the initial value of  $\theta$  at the beginning of the wake†.

*3.5 Wake.*—Near the trailing edge of an aerofoil it is likely that the assumption of the boundary layer theory that the pressure gradient across the layer is negligible is invalid. But the pressure gradient across the wake will become small a short distance downstream of the trailing edge and the approximations of boundary layer theory will therefore again become valid. It will be assumed that the theory can be used to investigate the flow downstream of the trailing edge; the modifications required to allow for pressure gradients across the boundary layer and the wake are considered in Appendix III.

At the trailing edge of an aerofoil the pressure is higher than in the free stream and it falls steadily downstream from the trailing edge. At the same time the wake becomes broader owing to turbulent mixing so that  $H$ , the ratio of the displacement thickness to the momentum thickness, falls from its value at the trailing edge to the value unity far downstream.

The momentum equation of the wake has the same form as (7) or (8) for a boundary layer, except that the surface friction  $\tau_0$  is zero; for the wake equation (8) therefore becomes

$$\frac{d\theta}{dx} + \frac{U'}{U} (H + 2) \theta = 0 \quad \dots \quad \dots \quad \dots \quad \dots \quad (12)$$

where  $x$  is now measured downstream along the centre line of the wake,  $U$  is the velocity at the edge of the wake, and  $\theta$  is the momentum thickness of the wake, which arises from the boundary layers of both surfaces of the aerofoil. Equation (12) may be written

$$\frac{1}{\theta} \frac{d\theta}{dx} = - (H + 2) \frac{d}{dx} \left[ \log_e \frac{U}{U_0} \right]$$

where  $U_0$  is the velocity of the stream at infinity.

\* It is advisable in solving (11) to use non-dimensional quantities by measuring distances as fractions of the chord  $c$ , velocities as fractions of the stream velocity  $U_0$ , and replacing  $v$  by  $1/R$ .

† It has been shown by Betz<sup>9</sup> that the values of  $U$  on the upper and lower surfaces are equal at the trailing edge.

Integrating this equation from the trailing edge to infinity we obtain, after integration by parts,

$$\left[ \log \theta \right]_{\infty}^{\text{T.E.}} = - \left[ (H + 2) \log \frac{U}{U_0} \right]_{\infty}^{\text{T.E.}} + \int_{\infty}^{\text{T.E.}} \log \frac{U}{U_0} \cdot \frac{dH}{dx} \cdot dx$$

This gives

$$\log \frac{\theta_1}{\theta_0} + (H_1 + 2) \log \frac{U_1}{U_0} = \int_1^{H_1} \log \frac{U}{U_0} \cdot dH$$

where at the trailing edge

$$\theta = \theta_1, \quad U = U_1, \quad H = H_1,$$

and at infinity downstream

$$\theta = \theta_0, \quad U = U_0, \quad H = 1.$$

Hence

$$\theta_0 = \theta_1 \left( \frac{U_1}{U_0} \right)^{H_1 + 2} \exp \left[ \int_1^{H_1} \log \frac{U_0}{U} dH \right] \dots \dots \quad (13)$$

In order to evaluate the integral on the right hand side of (13) it is necessary to find a relation between the wake pressure, which is related to  $U$  by Bernouilli's equation, and the velocity distribution in the wake, which is related to  $H$ . We note first that  $\log(U_0/U)$  decreases continuously from its value  $\log(U_0/U_1)$  at the trailing edge to zero at infinity, while  $H$  decreases continuously from its value  $H_1$  at the trailing edge to the value unity at infinity; hence

$$0 < \int_1^{H_1} \log \frac{U_0}{U} dH < (H_1 - 1) \log \frac{U_0}{U_1}$$

and

$$1 < \exp \left[ \int_1^{H_1} \log \frac{U_0}{U} dH \right] < \left( \frac{U_0}{U_1} \right)^{H_1 - 1}$$

It has been assumed that the value of  $H$  in the turbulent boundary layer is equal to 1.4 so that we may take  $H_1 = 1.4$ . In addition the values of  $U_0/U_1$  for the two aerofoils considered are 1.11 and 1.28 (see Fig. 2 and 3), so that for the thinner section

$$\left. \begin{aligned} 0 &< \int_1^{H_1} \log \frac{U_0}{U} dH < 0.046, \\ 1 &< \exp \left[ \int_1^{H_1} \log \frac{U_0}{U} dH \right] < 1.046, \end{aligned} \right\}$$

and for the thicker section

$$1 < \exp \left[ \int_1^{H_1} \log \frac{U_0}{U} dH \right] < 1 \cdot 10$$

The range of possible values of the last factor in (13) is therefore small and we shall be justified in making a rough approximation to its value.

The only available experimental data to determine the relation between  $U_0/U$  and  $H$  are given in Reference 10, in which explorations in flight of flow in the wake of a wing at various distances from the trailing edge are described\*. The results

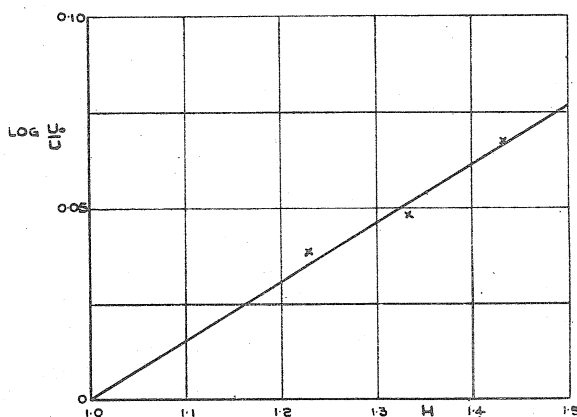


FIG. 4.—Relation between  $\log_e U_0/U$  and  $H$  in the Wake of an Aerofoil.  
 × Experimental Results.

deduced from Fig. 11-13 of this report are given in Fig. 4, and show that the relation between  $H$  and  $\log U_0/U$  is given approximately by the formula

$$\frac{\log U_0/U}{H - 1} = \text{constant}$$

It will be assumed that this linear relation holds generally, so that we put

$$\frac{\log U_0/U}{\log U_0/U_1} = \frac{H - 1}{H_1 - 1}$$

Hence

$$\int_{-1}^{H_1} \log \frac{U_0}{U} dH = \frac{H_1 - 1}{2} \log \frac{U_0}{U_1}$$

and then

$$\exp \left[ \int_1^{H_1} \log \frac{U_0}{U} dH \right] = \left( \frac{U_0}{U_1} \right)^{\frac{H_1 - 1}{2}} \quad \dots \quad \dots \quad \dots \quad (14)$$

\* Wind tunnel measurements are unreliable owing to the possible presence of static pressure gradients in the main stream.

Substituting from (14) equation (13) becomes

$$\theta_0 = \theta_1 \left( \frac{U_1}{U_0} \right)^{\frac{H_1+5}{2}} \quad \dots \quad \dots \quad \dots \quad \dots \quad \dots \quad (15)$$

and, with  $H_1 = 1.4$ ,

$$\theta_0 = \theta_1 \left( \frac{U_1}{U_0} \right)^{3.2}$$

The drag coefficient of the aerofoil is then, from (3),

$$C_D = \frac{2\theta_0}{c} = \frac{2\theta_1}{c} \left( \frac{U_1}{U_0} \right)^{3.2} \quad \dots \quad \dots \quad \dots \quad \dots \quad (16)$$

In concluding this section it may be pointed out that the above analysis of the wake may be applied to derive an alternative formula for determining the drag of a wing from wake explorations. If (12) is integrated from some position downstream of the trailing edge to infinity, instead of from the trailing edge itself, we obtain

$$\theta_0 = \theta_2 \left( \frac{U_2}{U_0} \right)^{H_2+2} \exp \left[ \int_1^{H_2} \log \frac{U_0}{U} dH \right] \quad \dots \quad \dots \quad (17)$$

where the suffix 2 denotes that values at the exploration plane are to be taken. Equation (17) is exact and it may be shown as before that

$$0 < \int_1^{H_2} \log \frac{U_0}{U} dH < (H_2 - 1) \log \frac{U_0}{U_2}$$

which gives a small range of possible values of the integral.

If the value of this integral is approximated to in the same way as before, we obtain for the drag coefficient of the body

$$C_D = \frac{2\theta_0}{c} = \frac{2\theta_2}{c} \left( \frac{U_2}{U_0} \right)^{\frac{H_2+5}{2}} \quad \dots \quad \dots \quad \dots \quad \dots \quad (18)$$

This formula takes the development of the wake downstream of the measurement plane into account more correctly than do the formulae of Betz<sup>11</sup> and Jones<sup>10</sup>. It is less satisfactory than these formulae, however, in that it can only be applied directly if the pressure in the wake at the measurement plane may be taken as constant\*. The numerical values for drag given by (18) generally differ only slightly from the values given by Jones's formula.

*4. Details of calculations.* 4.1. *Cases considered.*—It was desired to cover a sufficient number of cases to enable interpolations to be made for the profile drag of aerofoils for a range of wing thickness, Reynolds number and transition point positions. The effect of roughness is not considered, though this could be examined by a modification of the method used. Other factors are lift coefficient and section shape; but since the profile drag of wings is important mainly at top speed and experiments indicate that the drag of a good section does not vary much over a

---

\* See Appendix III.

range of lift coefficient, provided that the lift coefficient is small, only a single value of the lift coefficient is considered; also the variation in drag with section shape\* is probably small and only one wing section is considered for each thickness.

In addition to the flat plate the aerofoils of thickness  $0 \cdot 14c$  and  $0 \cdot 25c$ , shown inset in Fig. 2 and 3, were considered. These aerofoils were chosen because flight experiments on the drag of these sections were proceeding and it was desired to compare the theoretical results with experiment.

The drag was calculated for Reynolds numbers of  $10^6$ ,  $10^7$  and  $5 \times 10^7$ . The lowest Reynolds number was chosen to correspond roughly with atmospheric wind tunnel tests, the next to correspond with flight experiments at the Royal Aircraft Establishment and at Cambridge, and the last as representing the highest likely to be attained on aeroplanes in the next few years.

The effect on drag of transition point position was investigated by considering transition point positions on the upper and lower surfaces near the leading edge and at distances of about  $0 \cdot 2c$  and  $0 \cdot 4c$  from the leading edge†. In the slipstream transition occurs close to the leading edge<sup>12</sup> and flight tests<sup>2, 7</sup> have shown that, outside the slipstream, transition may occur at distances up to  $0 \cdot 4c$  back from the leading edge.

TABLE 2

Thickness chord.	Reynolds number.	Distance of T.P. behind the L.E. (Top surface).	Distance of T.P. behind the L.E. (Bottom surface).	$C_D$ (Top surface).	$C_D$ (Bottom surface).	$C_f$ (Top surface).	$C_f$ (Bottom surface).
0	$10^6$	0	0	0.00461	0.00461	0.00461	0.00461
0	$10^6$	$0 \cdot 2c$	$0 \cdot 2c$	0.00411	0.00411	0.00411	0.00411
0	$10^6$	$0 \cdot 4c$	$0 \cdot 4c$	0.00356	0.00356	0.00356	0.00356
0	$10^7$	0	0	0.00300	0.00300	0.00300	0.00300
0	$10^7$	$0 \cdot 2c$	$0 \cdot 2c$	0.00259	0.00259	0.00259	0.00259
0	$10^7$	$0 \cdot 4c$	$0 \cdot 4c$	0.00211	0.00211	0.00211	0.00211
0	$5 \times 10^7$	0	0	0.00235	0.00235	0.00235	0.00235
0	$5 \times 10^7$	$0 \cdot 2c$	$0 \cdot 2c$	0.00197	0.00197	0.00197	0.00197
0	$5 \times 10^7$	$0 \cdot 4c$	$0 \cdot 4c$	0.00158	0.00158	0.00158	0.00158
$0 \cdot 14$	$10^6$	$0 \cdot 017c$	$0 \cdot 03c$	0.00725	0.00585	0.00565	0.00489
$0 \cdot 14$	$10^6$	$0 \cdot 177c$	$0 \cdot 177c$	0.00653	0.00504	0.00524	0.00431
$0 \cdot 14$	$10^6$	$0 \cdot 376c$	$0 \cdot 376c$	0.00521	0.00405	0.00431	0.00346
$0 \cdot 14$	$10^7$	$0 \cdot 017c$	$0 \cdot 03c$	0.00477	0.00381	0.00375	0.00321
$0 \cdot 14$	$10^7$	$0 \cdot 177c$	$0 \cdot 177c$	0.00412	0.00312	0.00331	0.00274
$0 \cdot 14$	$10^7$	$0 \cdot 376c$	$0 \cdot 376c$	0.00309	0.00234	0.00256	0.00211
$0 \cdot 14$	$5 \times 10^7$	$0 \cdot 017c$	$0 \cdot 03c$	0.00375	0.00298	0.00290	0.00248
$0 \cdot 14$	$5 \times 10^7$	$0 \cdot 177c$	$0 \cdot 177c$	0.00316	0.00236	0.00252	0.00210
$0 \cdot 14$	$5 \times 10^7$	$0 \cdot 376c$	$0 \cdot 376c$	0.00230	0.00172	0.00192	0.00158
$0 \cdot 25$	$10^6$	$0 \cdot 034c$	$0 \cdot 024c$	0.01048	0.00764	0.00653	0.00553
$0 \cdot 25$	$10^6$	$0 \cdot 189c$	$0 \cdot 196c$	0.00911	0.00661	0.00593	0.00499
$0 \cdot 25$	$10^6$	$0 \cdot 386c$	$0 \cdot 396c$	0.00668	0.00501	0.00457	0.00388
$0 \cdot 25$	$10^7$	$0 \cdot 034c$	$0 \cdot 024c$	0.00690	0.00503	0.00431	0.00366
$0 \cdot 25$	$10^7$	$0 \cdot 189c$	$0 \cdot 196c$	0.00572	0.00412	0.00370	0.00310
$0 \cdot 25$	$10^7$	$0 \cdot 386c$	$0 \cdot 396c$	0.00378	0.00286	0.00265	0.00228
$0 \cdot 25$	$5 \times 10^7$	$0 \cdot 034c$	$0 \cdot 034c$	0.00545	0.00403	0.00335	0.00285
$0 \cdot 25$	$5 \times 10^7$	$0 \cdot 189c$	$0 \cdot 196c$	0.00435	0.00312	0.00281	0.00236
$0 \cdot 25$	$5 \times 10^7$	$0 \cdot 386c$	$0 \cdot 396c$	0.00274	0.00208	0.00196	0.00168

\* The transition point positions may, however, be affected by shape of section and lift coefficient; see Appendix II.

† Measured parallel to the chord.

4.2. *Results of calculations.*—The numerical results are given in Table 2, which shows the contributions to  $C_D$  and  $C_f$  from the upper and lower surfaces separately. Fig. 5-7 show the profile drag results for the complete aerofoils plotted against wing thickness for the same locations of the transition points on both surfaces\*.

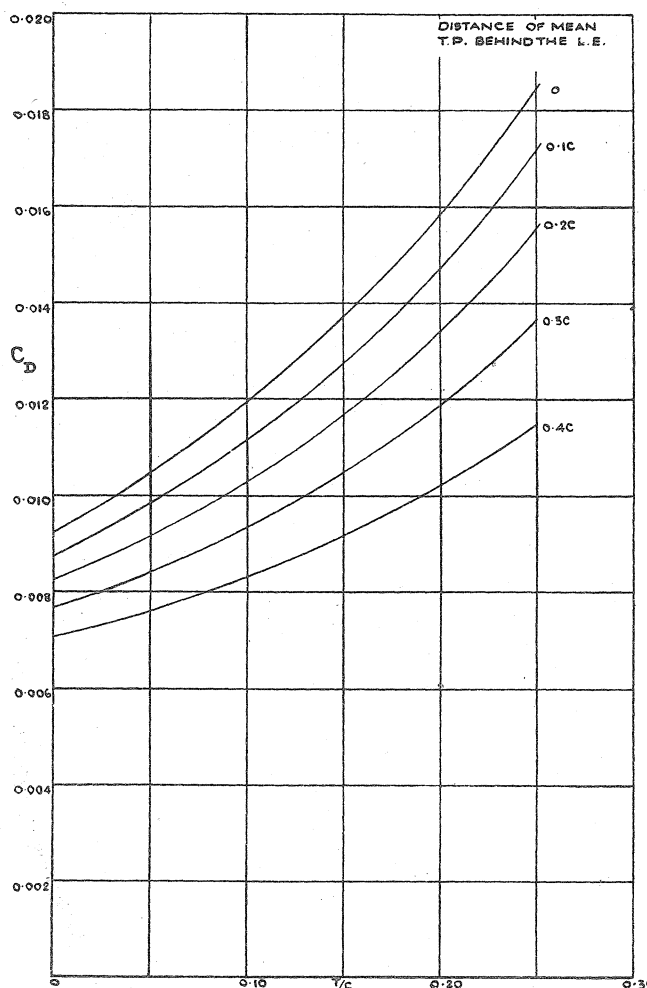


FIG. 5.—Variation of Calculated Profile Drag Coefficient with Wing Thickness and Position of Mean Transition Point.  $R = 10^6$ .

The results have been cross-plotted for simplicity in use and are given again in Fig. 8-12, in which the drag coefficient is plotted against Reynolds number for various wing thicknesses, each figure corresponding to a given mean transition point position, measured parallel to the chord from the leading edge.

\* In using the curves to estimate the drag of an aerofoil with different transition point positions on the two surfaces, it is sufficiently accurate to assume that the transition points are both situated at their mean position, midway between their actual positions on the two surfaces. This is permissible as the variation of the drag of either surface with variation of transition point position is roughly linear and much the same for both surfaces.

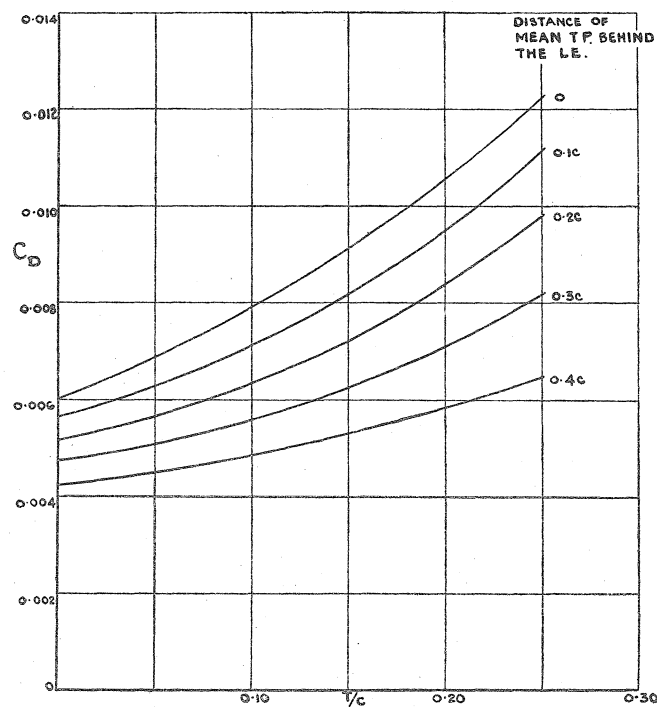


FIG. 6.—Variation of Calculated Profile Drag Coefficient with Wing Thickness and Position of Mean Transition Point.  $R = 10^7$ .

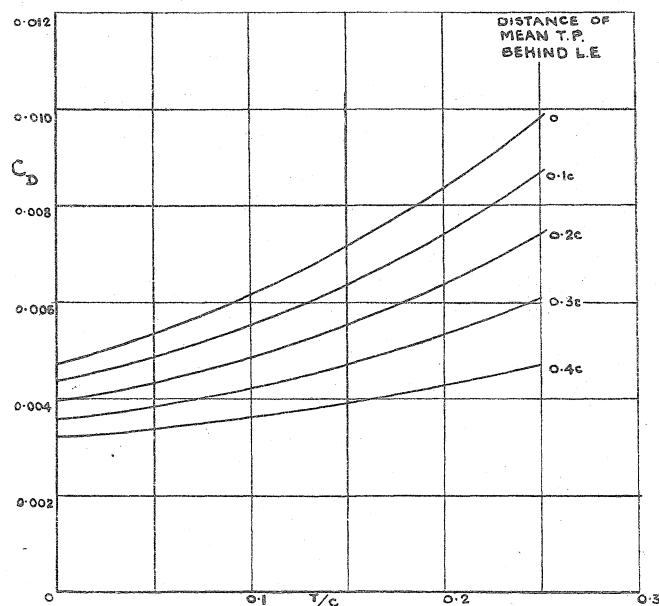


FIG. 7.—Variation of Calculated Profile Drag Coefficient with Wing Thickness and Position of Mean Transition Point.  $R = 5 \times 10^7$ .

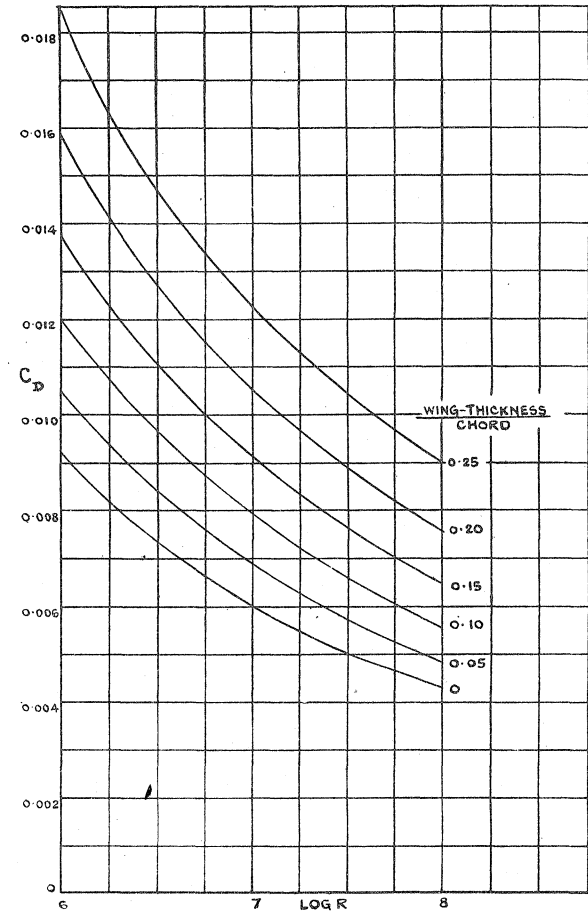


FIG. 8.—Variation of Profile Drag with Reynolds Number and Wing Thickness. Transition Points at the Leading Edge.

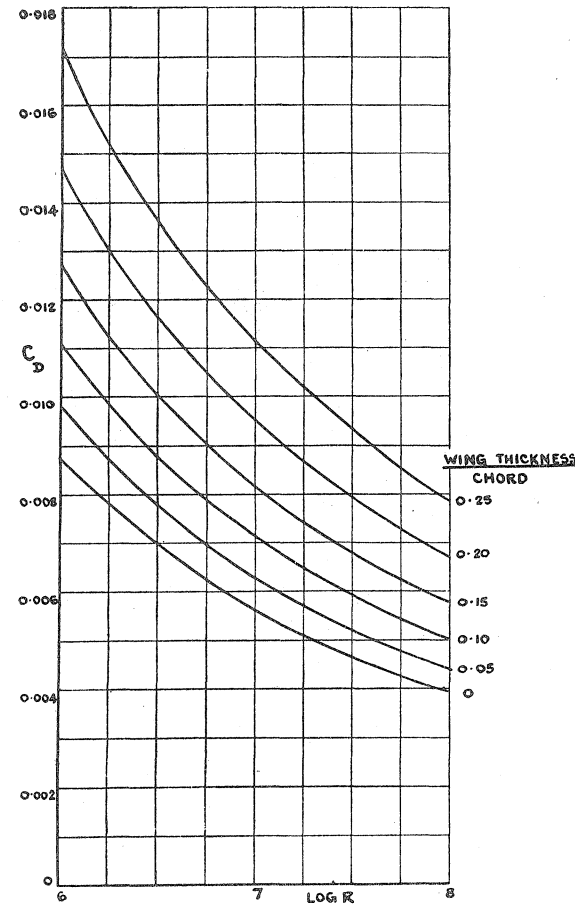


FIG. 9.—Variation of Profile Drag with Reynolds Number and Wing Thickness. Transition Points at  $0.1c$  behind the Leading Edge.

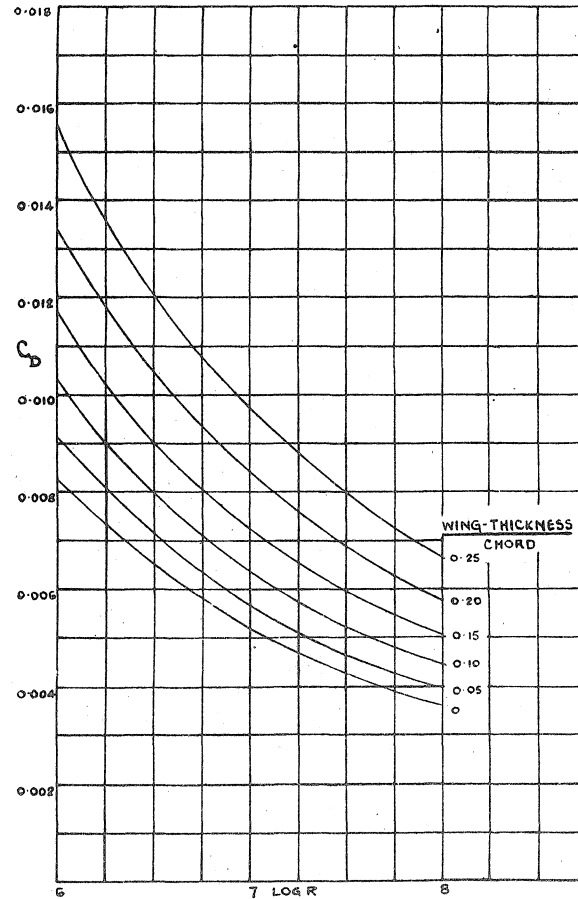


FIG. 10.—Variation of Profile Drag with Reynolds Number and Wing Thickness. Transition Points at  $0.2c$  behind the Leading Edge.

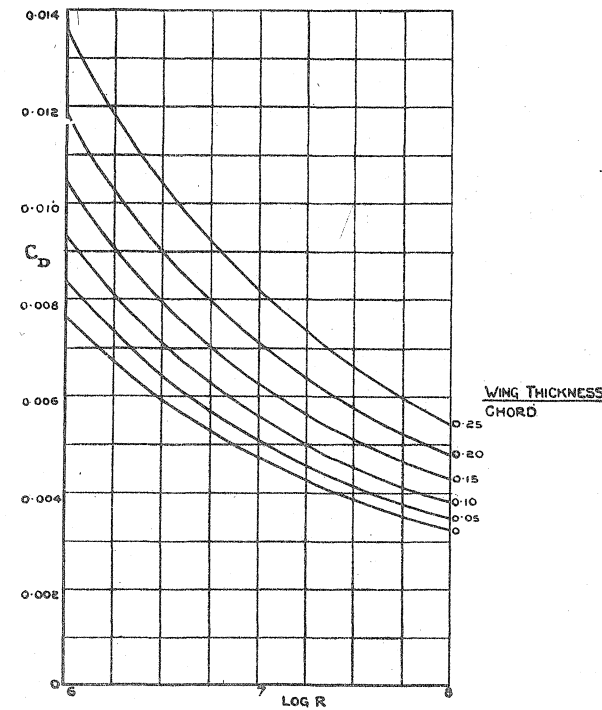


FIG. 11.—Variation of Profile Drag with Reynolds Number and Wing Thickness. Transition Points at  $0.3c$  behind the Leading Edge.

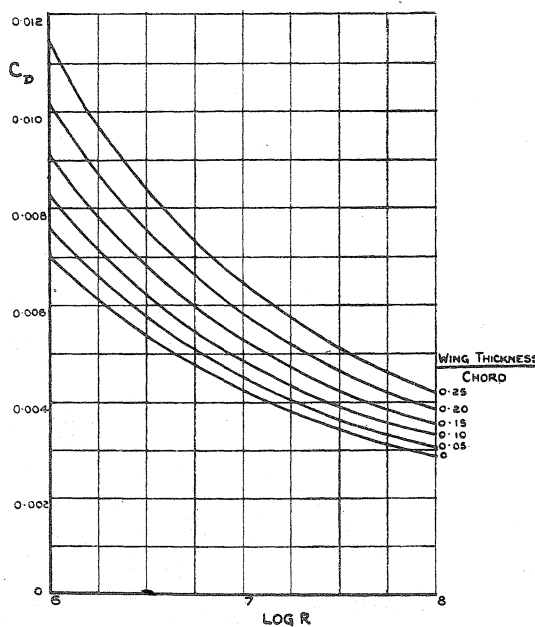


FIG. 12.—Variation of Profile Drag with Reynolds Number and Wing Thickness.  
Transition Points at  $0.4c$  behind the Leading Edge.

An example of the type of skin friction distributions obtained is given in Fig. 13 which shows  $c_f (= 2\tau_0/\rho U_0^2)$  plotted against distance along the wing chord from

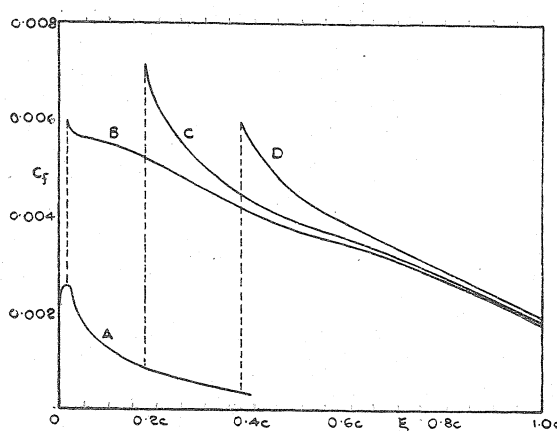


FIG. 13.—Skin Friction Distribution on Upper Surface of 14 per cent. Thick Wing for  $R = 10^7$ .

- A — Laminar flow.
- B — Turbulent Flow, Transition Point at  $\xi = 0.017c$ .
- C — Turbulent Flow, Transition Point at  $\xi = 0.177c$ .
- D — Turbulent Flow, Transition Point at  $\xi = 0.376c$ .

the leading edge for the thinner aerofoil (Fig. 2) for  $R = 10^7$ , for three transition point positions. Fig. 14 shows the variations of profile drag coefficient  $C_D$  and skin friction drag coefficient  $C_f$  for the thinner aerofoil (both surfaces), for  $R = 10^7$

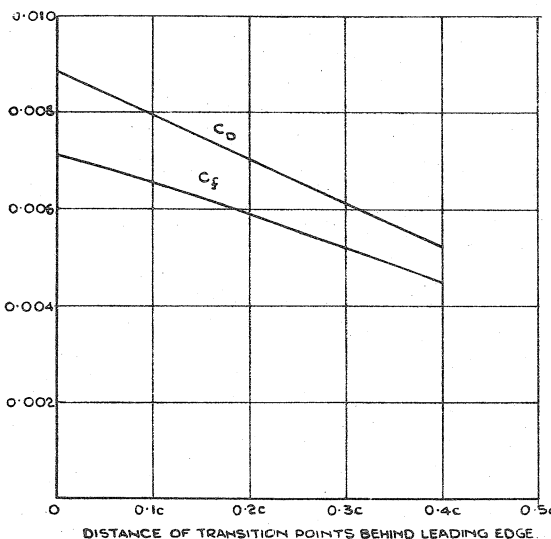


FIG. 14.—Variation of Profile Drag and Skin Friction with Transition Point Position for 14 per cent. Thick Wing for  $R = 10^7$ .

with variation of mean transition point position. The difference between  $C_D$  and  $C_f$  in Fig. 14 is presumably due to form drag, which appears as the component of the normal pressures along the direction of flight. The variation of the ratios skin friction drag/profile drag and form drag/profile drag plotted against aerofoil thickness for various transition point positions is shown in Fig. 15; these ratios

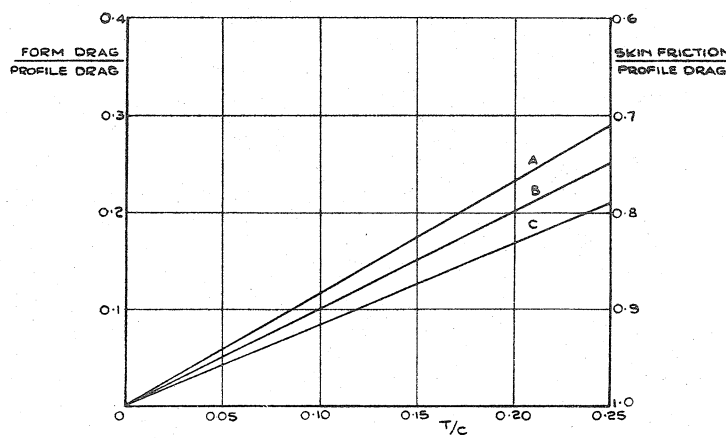


FIG. 15.—Variation of Form Drag and Skin Friction with Wing Thickness.

- A — Transition Points at Leading Edge.
- B — Transition Points at  $0.2c$ .
- C — Transition Points at  $0.4c$ .

were found to be independent of Reynolds number to the order of accuracy of the calculations. It will be seen that the ratio form drag/profile drag increases linearly with wing thickness and decreases slowly with backward movement of the transition point.

**4.3. Accuracy.**—The accuracy of the method of solution of the equations cannot easily be estimated as each case involves a step-by-step integration of a differential equation, but it is likely that the arithmetical errors are less than 1 per cent.

It is considered that Pohlhausen's method will be quite accurate for the determination of the momentum thickness of the boundary layer at the transition point. The assumption of a sudden transition to turbulence will introduce errors which will be small if the transition region is short ; it is estimated that a transition region extending over  $0.05c$  may introduce an error of about 3 per cent.

The error due to the use of (9) to relate  $\theta$  and  $\tau_0$ , the equation being derived by neglecting the effect of the pressure gradient on the velocity distribution in the turbulent boundary layer, cannot be determined owing to lack of experimental data. It seems likely, however, that for wings at small lift coefficients, for which the pressure gradients are much smaller than the pressure gradients which are sufficient to cause separation, the velocity distribution in the turbulent boundary layer of an aerofoil will not differ greatly from the velocity distribution in the turbulent boundary layer of a flat plate.

Errors may arise from inaccuracies in the assumed pressure distributions, particularly as the pressure distribution near the trailing edge has been faired in to allow roughly for the effect of the thick boundary layer on the pressure distribution ; it has also been assumed that the effect of lift coefficient and of profile shape on drag is small. The first of these points was tested by replacing the velocity distribution for the thicker aerofoil over the rear 20 per cent. of the chord by the curve shown dotted in Fig. 3. The profile drag and skin friction were calculated with this modified pressure distribution for  $R = 10^7$  and it was found that the profile drag was increased by about 2 per cent. and the skin friction decreased by the same amount. It may be concluded that the calculated drag is insensitive to small changes in the assumed pressure distribution.

It has also been assumed that the value of  $H$  in the turbulent boundary layer may be taken to be 1.4 ; but it is probable that  $H$  becomes greater than 1.4 towards the trailing edge. To test the effect of variations in  $H$ , the profile drag and skin friction were calculated for the thicker aerofoil (Fig. 3) for  $R = 10^7$ , assuming that  $H$  increases uniformly from 1.4 to 1.8 over the last 20 per cent. of the chord,  $H$  decreasing again from 1.8 to unity in the wake. The effect of this was to increase the profile drag by about 1 per cent., the skin friction drag changing by a negligible amount. It may therefore be concluded that variations in  $H$  from the value assumed have little effect on profile drag.

5. Comparison with experiment.—Comparison with experimental results can only be made satisfactorily if the drag and the transition points on both surfaces have been measured.

The results obtained for a 25 per cent. thick wing tested on the Hawcon<sup>2</sup>, and the results obtained at Cambridge\* on wings of 10·5 per cent.<sup>†</sup> and 17·5 per cent. thickness are given in Table 3. Experiments made on a Battle with a 17 per cent.

TABLE 3

Wing thickness chord.	Reynolds number.	$C_L$	Position of transition points.		Measured $C_D$	Calculated $C_D$
			Upper surface.	Lower surface.		
0·25	$6\cdot1 \times 10^6$	0·45	0·34c	0·37c	0·0080	0·0031
0·25	$8\cdot2 \times 10^6$	0·25	0·36c	0·30c	0·0050	0·0079
0·105	$5\cdot4 \times 10^6$	0·30	0·28 <sup>5</sup> c	0·25 <sup>5</sup> c	0·0039	0·0037
0·175	$5\cdot2 \times 10^6$	0·37	0·36 <sup>5</sup> c	0·16 <sup>5</sup> c	0·0079	0·0030

thick wing, on which the transition points were fixed by thin spanwise wires at 0·10c and 0·05c on the upper and lower surfaces respectively, are compared with the theoretical results in Fig. 16. The agreement between theory and experiment is quite satisfactory in all cases. It should be remarked, however, that the location of transition points by the creeper method<sup>7</sup>, which measures the rate of growth of the boundary layer in the transition region, is to some extent arbitrary and that

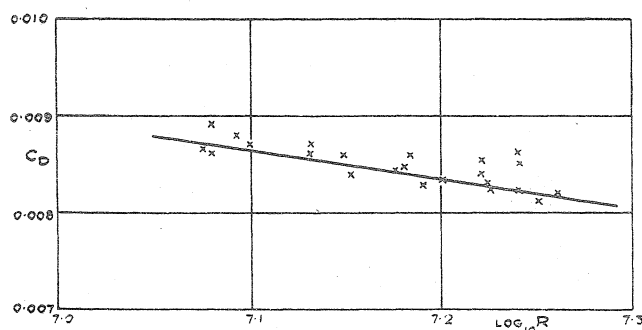


FIG. 16.—Comparison between Theory and Experiment for Drag of 17 per cent. Thick Wing with Transition Points at 0·10c and 0·05c on Upper and Lower Surfaces respectively.

— Theory.

× Experimental Points.

\* Communicated by Mr. A. V. Stephens.

† The 10·5 per cent. thick wing was the lower wing of a biplane and so was subject to some interference from the upper wing.

a different method of determining the transition points might lead to different locations. This effect is unlikely to be very important in flight tests for which the transition region is short, but may be important in wind tunnel experiments, for which the transition region may be extensive.

*6. Extensions of the theory.*—The method of calculating the profile drag of smooth aerofoils may be applied to other problems if some modifications are made. For example, the drag of rough aerofoils can be determined if equation (9) is replaced by a formula which includes the effect of roughness ; for fully developed roughness flow (9) is replaced by

$$\zeta = \text{constant},$$

the value of the constant chosen depending on the magnitude of the roughness. The momentum equation retains the form (8).

The method may also be applied to calculate the drag of streamline bodies with axes along the stream. The laminar boundary layer may be analysed by Tomotika's method<sup>13</sup>. For the turbulent boundary layer (9) is still valid but the momentum equation (8) must be replaced by

$$\frac{d\theta}{dx} + \left[ \frac{U'}{U} (H + 2) + \frac{r'}{r} \right] \theta = \frac{\tau_0}{\rho U^2}$$

where  $r$  is the radius of a section normal to the stream at a distance  $x$  from the nose (measured along the surface). Modifications are, however, necessary for the rear part of the body where  $r$  is small and, in addition, the analysis of the wake must be modified.

## 7. APPENDIX I

*Derivation of equation (9).*—The functional form of the relation between  $\theta$  and  $\zeta$  represented by (9) was derived from Karman's formula<sup>14</sup> for the local surface friction at a point distance  $x$  from the leading edge of a flat plate with fully turbulent boundary layer, which may be written

$$\zeta = A + B \log_e \left( \frac{Ux}{\nu} \cdot \frac{1}{\zeta^2} \right) \quad \dots \dots \dots \dots \dots \quad (19)$$

where

$$\zeta^2 = \rho U^2 / \tau_0$$

and A and B are constants.

For a flat plate the momentum equation (8) becomes

$$\frac{d\theta}{dx} = \frac{1}{\zeta^2} \quad \dots \dots \dots \dots \dots \dots \quad (20)$$

If we substitute for  $x$  from (19) in (20) and integrate, the relation

$$\frac{U\theta}{\nu} = C(eD\zeta - 1) \quad \dots \dots \dots \dots \dots \dots \quad (21)$$

is derived, where C and D are constants (which depend on A and B), the constant of integration is obtained from the condition that  $\theta$  and  $\zeta$  vanish together at the leading edge of the plate, and some terms of lower order than those retained have been omitted. The second term on the right hand side of (21) may be omitted since  $eD\zeta$  is a large quantity except near the leading edge, so that (21) becomes

$$\frac{U\theta}{\nu} = C eD\zeta \quad \dots \dots \dots \dots \dots \dots \quad (22)$$

The constants C and D were not determined directly from the numerical values of A and B, owing to the omission of some second order terms, but were chosen to give the best agreement with the accepted formula

$$C_D = 0.455 (\log_{10} R)^{-2.58} \quad \dots \dots \dots \dots \dots \dots \quad (23)$$

for the drag of a flat plate with fully turbulent boundary layer.

Substituting for  $\theta$  from (21) or (22) in (20) and integrating, we obtain

$$\frac{Ux}{\nu} = C eD\zeta \left( \zeta^2 - \frac{2}{D} \zeta + \frac{2}{D^2} \right) - \frac{2C}{D^2} \quad \dots \dots \dots \quad (24)$$

the constant of integration being determined by the condition that  $x$  and  $\zeta$  vanish together at the leading edge of the plate. For any values of C and D and of  $R = Uc/\nu$ , equation (24) may be solved numerically for  $\zeta$  after putting  $x = c$ . The corresponding value of  $\theta$  at the trailing edge is given by (22) and the drag coefficient of the plate, taking account of both sides, is\*

$$C_D = \frac{4\theta}{c} \quad \dots \dots \dots \dots \dots \dots \quad (25)$$

TABLE 4  
*Drag coefficient of flat plate*

$R$	$C_D$ given by (25)	$C_D$ given by (23)
$10^6$	0.00461	0.00445
$2 \times 10^6$	0.00402	0.00399
$5 \times 10^6$	0.00340	0.00340
$10^7$	0.00301	0.00301
$2 \times 10^7$	0.00270	0.00270
$5 \times 10^7$	0.00235	0.00235

\* This equation follows from (3), since the pressure at the trailing edge of a flat plate is equal to the pressure in the free stream.

It was found that  $C = 0.2454$  and  $D = 0.3914$  gave the best agreement between (23) and (25). The comparison is shown in Table 4 for these values of  $C$  and  $D$ . It will be seen that the differences are negligible for  $R > 2 \times 10^6$  but that there is a difference of  $3\frac{1}{2}$  per cent. for  $R = 10^6$ . It may be concluded that the formula

$$\frac{U\theta}{v} = 0.2454 e^{0.3914\xi}$$

represents the relation between  $\theta$  and  $\xi$  for the fully turbulent boundary layer of a flat plate with sufficient accuracy.

## 8. APPENDIX II

*Factors controlling transition.*—The analysis given in this report gives a satisfactory method of calculating profile drag provided that the positions of the transition points are known. The determination of a law governing transition presents considerable difficulties owing to the need to make experiments in flight or in wind tunnels of low turbulence. It is probable that turbulence is the major factor controlling transition in all wind tunnels which have not been specially designed to have extremely low turbulence. The turbulence in the atmosphere of a scale which may affect transition is negligible and flight experiments may be expected to throw most light on the factors governing transition. A comprehensive series of flight tests at Cambridge<sup>7</sup> has not, however, led to the formulation of a simple law; since an investigation of transition requires an analysis of the development of the laminar boundary layer, which in turn requires accurate differentiation of measured pressure distribution curves, it follows that the difficulty of interpreting flight tests is very great.

The flight tests at Cambridge and at Farnborough<sup>2</sup> do, however, indicate that for smooth surfaces transition to turbulence does not occur ahead of the pressure minimum. The experiments were all made at Reynolds numbers less than  $10^7$ , but the movement of the transition points with change of incidence is always in the same direction as the movement of the pressure minimum, so that the influence of the pressure gradients on transition may be regarded as established.

It is likely that transition on a wing at high Reynolds number will occur ahead of the laminar separation points and hence the location of these points is of considerable value in limiting the range of possible transition point positions. It is known that Pohlhausen's method cannot reliably be used to determine the laminar separation point, but a method developed by Howarth<sup>4</sup> seems to be satisfactory.

The view has been put forward by Dryden<sup>7</sup> that transition to turbulence in wind tunnels is due to the eddies causing local separation in the laminar layer, which in turn causes transition. If this view is correct it implies that transition to turbulence on smooth surfaces in flight is due to incipient separation of the laminar layer. An attempt was made to test this point for the 25 per cent. thick wing of the Hawcon<sup>2</sup> by calculating the laminar separation points by Howarth's method. The results indicated that the measured transition points on the upper surface were fairly close to the calculated separation points but that this did not hold for the lower surface; owing to the inaccuracy of the experimental pressure distribution the calculation is not considered to be reliable.

### 9. APPENDIX III

*Modifications to allow for pressure gradients across the boundary layer or wake.*—In the neighbourhood of the trailing edge of an aerofoil it is likely that the assumption that the pressure gradients across the boundary layers and the wake are negligible is invalid. The necessary modification to the momentum equation (7) or (8) due to this effect will be briefly considered here.

For steady flow the momentum equation may be written (see Reference 8, p. 107)

$$\frac{d}{dx} \int_0^h \rho u^2 dy - \rho U \int_0^h \frac{\partial u}{\partial x} dy = - \int_0^h \frac{\partial p}{\partial x} dy - \tau_0 \quad \dots \quad \dots \quad (26)$$

where  $h$  is some constant distance which is greater than the boundary layer thickness. If  $P$  is the pressure at  $y = h$ , which is related to  $U$  by Bernouilli's equation, we have

$$\begin{aligned} \frac{\partial p}{\partial x} &= \frac{dP}{dx} + \frac{\partial}{\partial x} (p - P) \\ &= - \rho U U' + \frac{\partial}{\partial x} (p - P) \end{aligned}$$

and (26) becomes

$$\frac{d}{dx} \int_0^h \rho u^2 dy - \rho U \frac{d}{dx} \int_0^h u dy + \int_0^h \rho U U' dy = - \frac{d}{dx} \int_0^h (p - P) dy - \tau_0$$

This may be reduced as in Reference 8 to

$$\tau_0 + \frac{d}{dx} \int_0^h (p - P) dy = \frac{d}{dx} \int_0^h \rho (U^2 - u^2) dy - \rho U \frac{d}{dx} \int_0^h (U - u) dy$$

or

$$\tau_0 = \frac{d}{dx} \left[ \rho U^2 \theta - \int_0^h (p - P) dy \right] + \rho U U' \delta^* \quad \dots \quad \dots \quad (27)$$

where, as before,

$$\theta = \int_0^h \frac{u}{U} \left( 1 - \frac{u}{U} \right) dy$$

and

$$\delta^* = \int_0^h \left( 1 - \frac{u}{U} \right) dy$$

Introducing a modified formula for the momentum thickness of the layer by the equation

$$\bar{\theta} = \theta - \int_0^h \frac{p - P}{\rho U^2} dy$$

equation (27) takes the form

$$\tau_0 = \frac{d \bar{\theta}}{dx} + \frac{U'}{U} (\bar{H} + 2) \bar{\theta}$$

where  $H = \delta^*/\theta$ . This is identical with (8) except for the substitutions of  $\bar{\theta}$  and  $\bar{H}$  for  $\theta$  and  $H$  respectively. The theory given in the text of the main report may therefore be applied in regions where the pressure gradient across the boundary layer or the wake is important, provided that the above substitutions are made. Small changes in the theoretical skin friction may result, but these would hardly affect the numerical results.

## 10. APPENDIX IV

*Notation*

- $x$  distance along surface from stagnation point or distance along centre line of wake.  
 $y$  distance measured normal to surface or normal to centre line of wake.  
 $\xi$  distance measured parallel to aerofoil chord from stagnation point.  
 $c$  chord of aerofoil.  
 $U_0$  velocity of undisturbed stream.  
 $U$  velocity at edge of boundary layer or wake.  
 $w$  velocity in boundary layer parallel to surface or in wake parallel to wake centre line.  
 $\delta$  boundary layer thickness.  
 $\delta^*$  displacement thickness of boundary layer or wake.  
 $\theta$  momentum thickness of boundary layer or wake.  
 $\theta_0$  momentum thickness of wake far downstream.  
 $H$   $\delta^*/\theta$ .  
 $C_D$  profile drag coefficient.  
 $C_f$  skin friction drag coefficient.  
 $c_f$  local skin friction coefficient  $(2 \tau_0 / \rho U_0^2)$ .  
 $\tau_0$  intensity of skin friction.  
 $z$   $\delta^2/\nu$ .  
 $\lambda$   $U' z$ .  
 $\zeta$   $(\rho U^2 / \tau_0)^{1/2}$ .  
 $F(\zeta) = 10 \cdot 411 \zeta^{-2} e^{-0 \cdot 3914 \zeta}$ .

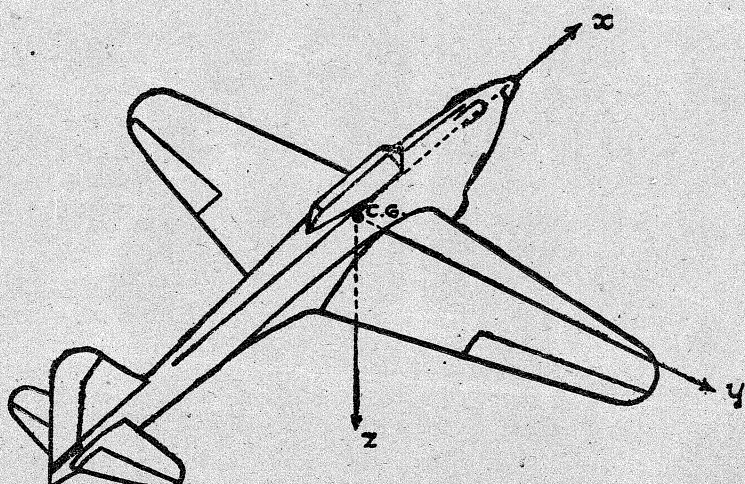
Suffix 1 denotes that quantities have their values at trailing edge.

Suffix 2 denotes that quantities have their values at an exploration plane in wake.

## LIST OF REFERENCES

No.	<i>Author.</i>	<i>Title, etc.</i>
1	Th. Theodorsen and I. E. Garrick	General potential theory of arbitrary wing sections. N.A.C.A. Report 452. 1933.
2	J. E. Serby, M. B. Morgan and E. R. Cooper	Flight tests on the profile drag of 14 per cent. and 25 per cent. thick wings. R. & M. 1826. 1937.
3	L. Howarth .. .. ..	Steady flow in the boundary layer near the surface of a cylinder in a stream. R. & M. 1632. 1934.
4	L. Howarth .. .. ..	On the solution of the laminar boundary layer equations. Proc. Roy. Soc. A.164 (1938), pp. 547-579.
5	A. Fage and V. M. Falkner ..	An experimental determination of the intensity of friction on the surface of an aerofoil. R. & M. 1315. 1930.
6	H. L. Dryden .. .. ..	Air flow in the boundary layer near a plate. N.A.C.A. Report 562. 1936.
7	B. M. Jones .. .. ..	Flight experiments on the boundary layer. Jour. Aero. Sciences, Vol. 5 (1938), pp. 81-101.
8	L. Prandtl .. .. ..	Aerodynamic theory (edited by Durand), Vol. 3, p. 108.
9	L. Howarth .. .. ..	The theoretical determination of the lift coefficient for a thin elliptic cylinder. Proc. Roy. Soc. A.149 (1935), pp. 558-586.
10	Cambridge University Aeronautics Laboratory.	Measurement of profile drag by the pitot-traverse method. R. & M. 1688. (1935-36.)
11	A. Betz .. .. ..	Z.F.M., Vol. 16 (1925), p. 42.
12	A. D. Young .. .. ..	Note on the effect of slipstream on boundary-layer flow. R.A.E. Report No. B.A. 1404. May, 1937. (Unpublished.)
13	S. Tomotika .. .. ..	The laminar boundary layer on the surface of a sphere in a uniform stream. R. & M. 1678. 1935.
14	Th. V. Karman .. .. ..	Turbulence and skin friction. Jour. Ae.Sc., Vol. 1 (1934), p. 1.

## SYSTEM OF AXES



Axes	Symbol Designation Positive direction	$x$ longitudinal forward	$y$ lateral starboard	$z$ normal downward
Force	Symbol	X	Y	Z
Moment	Symbol Designation	L rolling	M pitching	N yawing
Angle of Rotation	Symbol	$\phi$	$\theta$	$\psi$
Velocity	Linear Angular	$u$ $p$	$v$ $q$	$w$ $r$
Moment of Inertia		A	B	C

Components of linear velocity and force are positive in the positive direction of the corresponding axis.

Components of angular velocity and moment are positive in the cyclic order  $y$  to  $z$  about the axis of  $x$ ,  $z$  to  $x$  about the axis of  $y$ , and  $x$  to  $y$  about the axis of  $z$ .

The angular movement of a control surface (elevator or rudder) is governed by the same convention, the elevator angle being positive downwards and the rudder angle positive to port. The aileron angle is positive when the starboard aileron is down and the port aileron is up. A positive control angle normally gives rise to a negative moment about the corresponding axis.

The symbols for the control angles are :—

- $\xi$  aileron angle
- $\eta$  elevator angle
- $\eta_T$  tail setting angle
- $\zeta$  rudder angle